JOURNAL OF GEOPHYSICAL RESEARCH, VOL. 113, C07017, doi:10.1029/2007JC004241, 2008

Click Here for Full Article

Cross-shelf transport of freshwater on the New Jersey shelf

Renato Castelao,[1] Oscar Schofield,[1] Scott Glenn,[1] Robert Chant,[1] and Josh Kohut[1]

Received 22 March 2007; revised 13 January 2008; accepted 5 March 2008; published 16 July 2008.

[1] Repeated hydrographic surveys off New Jersey about 100 km south of the Hudson River mouth were conducted during spring and summer 2006. Glider observations reveal a strong seasonal variation in the surface salinity. Buoyant water is restricted to an area close to the coast during spring, but spans the entire shelf width during summer. During late July and August, freshwater lenses with large density anomaly are found up to 100 km from the coast. Surface velocity maps, satellite imagery and drifters' trajectories revealed the existence of a jet directed offshore and to the south, from near the river mouth toward the study region. This provides a direct pathway for transporting freshwater and any biogeochemical material it contains, including phytoplankton, dissolved organic and nonalgal particulate matter, across the shelf. The highest frequency of observation of the freshwater lenses offshore occurs when the jet transport is large, and the river discharge is relatively high. The transport in the jet is correlated with upwelling winds on scales of a few days.

Citation: Castelao, R., O. Schofield, S. Glenn, R. Chant, and J. Kohut (2008), Cross-shelf transport of freshwater on the New Jersey shelf, *J. Geophys. Res.*, *113*, C07017, doi:10.1029/2007JC004241.

1. Introduction

[2] Freshwater plumes derived from river sources are common features on the continental shelf. Generally, in the absence of ambient currents and if the spatial scale is large enough so that the Earth's rotation is important, river plumes turn to the right (left) in the northern (southern) hemisphere and flow in the direction of Kelvin wave propagation, forming a buoyancy-driven coastally trapped current [*Garvine*, 1995]. In the vicinity of the outflow, a bulge can be formed, which can be several times wider than the coastal current [e.g., *Yankovsky and Chapman*, 1997; *Avicola and Huq*, 2003; *Horner-Devine et al.*, 2006]. These nearshore coastal plumes can then flow tens to hundreds of kilometers alongshore before dispersing due to mixing with ambient shelf water [*Garvine*, 1999].

[3] Wind-forcing can substantially affect the dispersal of river plumes. Steady alongshore winds can advect the plume front either onshore or offshore in a manner consistent with Ekman dynamics [*Csanady*, 1978]. Downwelling favorable winds compress plumes against the coast [*Munchow and Garvine*, 1993; *Fong and Geyer*, 2001; *García Berdeal et al.*, 2002; *Lentz and Largier*, 2006; *Choi and Wilkin*, 2007], while upwelling favorable winds can retard or block the buoyant coastal current [*Lentz*, 1995] and cause the buoyant water to separate from the coast, spread offshore, and eventually disperse if the winds are strong enough [*Fong et al.*, 1997; *Hickey et al.*, 1998; *Rennie et al.*, 1999; *Fong and Geyer*, 2001; *Johnson et al.*, 2001; *Sanders and Garvine*, 2001; *García Berdeal et al.*, 2002; *Hallock and Marmorino*, 2002; *Johnson et al.*, 2003; *Lentz*, 2004; *Choi and Wilkin*, 2007]. This is especially true in surface-advected plumes [*Yankovsky and Chapman*, 1997], when the buoyant inflow remains in a thin surface layer and is thus highly responsive to wind-forcing and with decreased interactions with the bottom topography. Indeed, upwelling favorable wind-forcing is thought to be one of the primary mechanisms for the offshore dispersal of many buoyant coastal plumes. However, numerical simulations by *García Berdeal et al.* [2002] and *Fong and Geyer* [2002] indicate that ambient shelf currents can have a first order effect on surface advected plumes and insofar as these currents are topographically steered there may be an indirect interaction between topography and surface advected plumes.

[4] On the continental shelf off the New Jersey coast, the primary local source of freshwater is the Hudson River (Figure 1). The Hudson River discharge has a strong seasonal variation, with the maximum average discharge occurring during the spring freshet. The river flow becomes partially mixed with ocean water within the river and estuary by tides [*Blumberg et al.*, 1999; *Peters*, 1999; *Geyer et al.*, 2000; *Warner et al.*, 2005]. In addition to the Hudson River input, waters from the north flowing south in the Labrador Current are also thought to supply freshwater of Arctic origin to the region [*Chapman and Beardsley*, 1989], helping decrease the mean salinity in the surface layer.

[5] The coastal ocean off New Jersey has been extensively surveyed during spring and summer of 2006, as part of the Lagrangian Transport and Transformation Experiment (LaTTE), the Shallow Water 2006 Joint Experiment (SW06), and the ongoing Rutgers University Glider Endurance Line (RUEL) which began in 2003. LaTTE observations, which extend back to 2004, were focused in the region around the Hudson River mouth. *Chant et al.*

[1]Institute of Marine and Coastal Sciences, Rutgers University, New Brunswick, New Jersey, USA.

Copyright 2008 by the American Geophysical Union.
0148-0227/08/2007JC004241$09.00

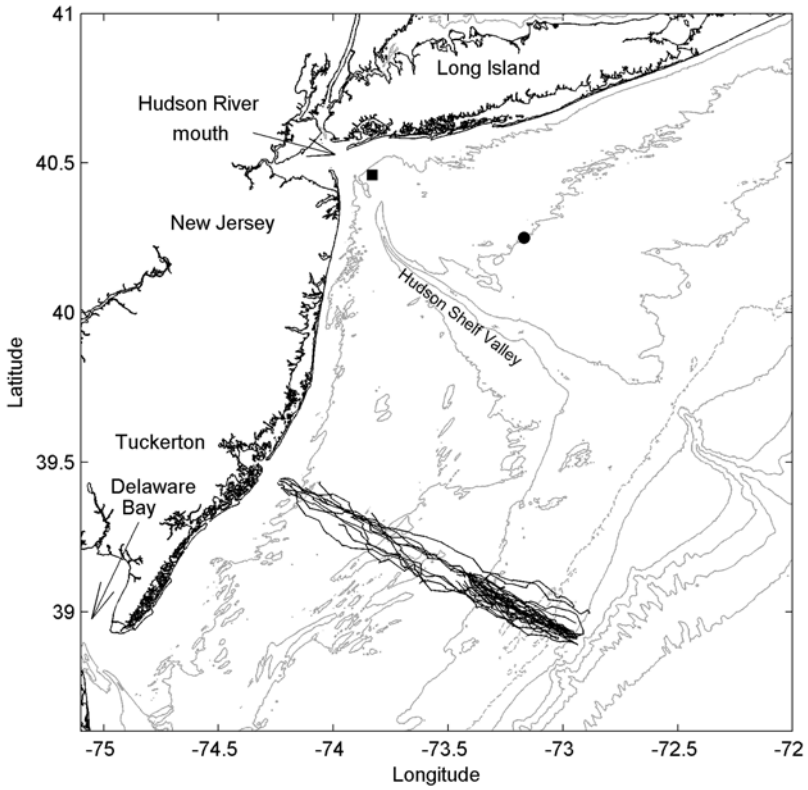

Figure 1. Study area showing glider tracks (black lines). Also shown are the locations of the NOAA NDBC buoy 44025 (circle) and CMAN station (square). Topographic contours shown are 20, 40, 60, 80 (dashed), 100, 200, 500, 1000, and 2000 m.

[2008] use those previous observations to describe details of the outflow in the vicinity of the mouth, including bulge formation and estimation of freshwater transport in the coastal current. The RUEL and the SW06 field efforts, on the other hand, were concentrated about 100 km south of the river mouth. In those cases, observations span the entire width of the shelf, although the region between the 60 and 100 m isobaths was more heavily sampled during SW06. In this paper, we make use of RUEL and SW06 observations to describe the freshwater content over the shelf in the south, away from the river mouth. After a description of the data collection and analyses methods (section 2), the hydrographic data are used to describe the seasonal evolution of the freshwater distribution over the shelf and to reveal the occurrence of freshwater lenses with high density anomaly in the offshore region, about 70–100 km from the coast (section 3.1). The remainder of the manuscript explores cross-shelf transport mechanisms that could explain those occurrences, in particular Ekman dynamics (section 3.2) and advection by an offshore directed jet (section 3.3). The results are discussed and conclusions are presented in section 4. The transport mechanisms of river plumes have important ecosystem implications, as they determine the extent of penetration of riverine material in the coastal ocean, including nutrients, estuarine species larvae and contaminants.

2. Data and Methods

[6] Repeated surveys of water over the shelf off New Jersey were conducted during spring and summer 2006, as part of SW06 and RUEL (Figure 1). The surveys were composed of cross-shelf sections up to 130 km long. RUEL observations generally extend from the 20 to the 100 m isobath, while observations during SW06 were more heavily concentrated in the region between the 60 and the 100 m isobaths. During SW06, glider transects were also obtained in other cross-sections both to the north and to the south of Tuckerton, NJ, although only observations along the Endurance Line are reported here.

[7] Hydrographic data were collected using a fleet of 8 Webb Research Corporation Slocum Coastal Electric Gliders [*Schofield et al.*, 2007], which cycle from surface to bottom while moving forward at an average speed of 24 km per day. The gliders are operational in water depths up to 200 m. All gliders are equipped with a Sea-Bird conductivity-temperature-depth (CTD) instrument. Typical along-track resolution is about 200 m near the shelf break improving to about 100 m over the shallower regions close to the coast. Measured and derived quantities (salinity, temperature, density; computed following *Fofonoff and Millard* [1983]) were gridded into vertical sections. For each glider transect, a straight line is fit to the actual vehicle location. Each variable (e.g., salinity) is then averaged onto that line vertically to 1 dbar bins and horizontally to 500 m. The use of autonomous vehicles (i.e., gliders) as the observational platform allowed for shelf waters to be observed relatively frequently over long periods of time. The Endurance Line (Figure 1) was sampled 34 times between early April and late September 2006.

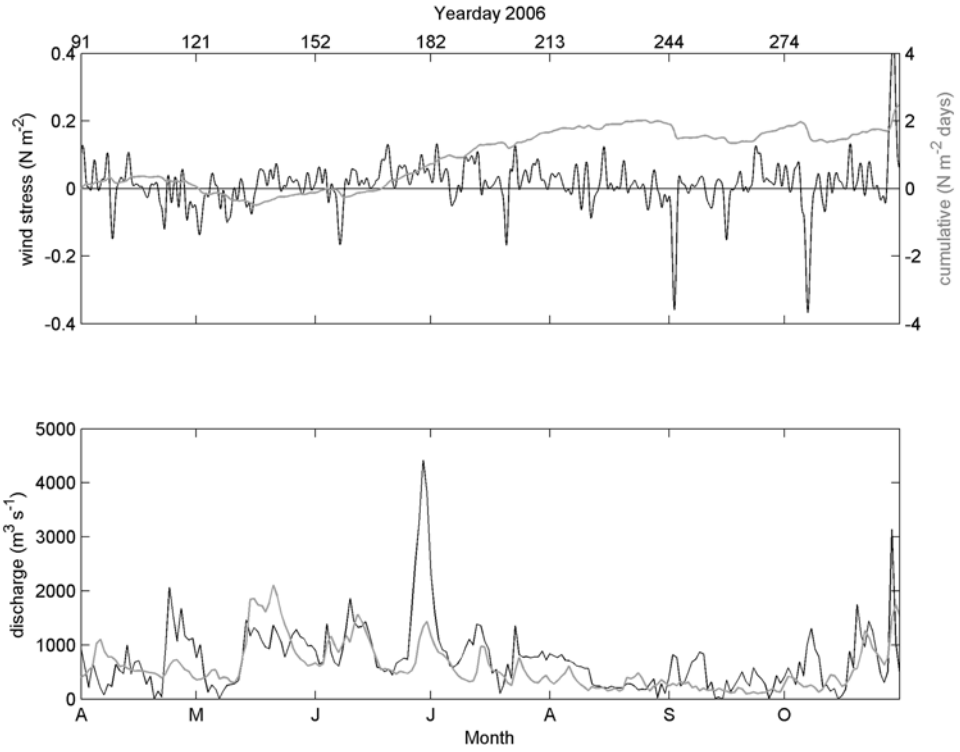

Figure 2. (top) Observed along-isobath component of the wind stress from NOAA NDBC buoy 44025 during 2006. Gray curve is cumulative wind stress starting at 1 April (day 91). Bottom shows the USGS measured Hudson River discharge at Poughkeepsie, NY in black, and the Connecticut River discharge at Thompsonville, CT in gray.

[8] Maps of surface currents were provided by an array of CODAR HF surface current mappers [*Barrick et al.*, 1977] consisting of four long-range and two high-resolution backscatter systems, which spans the New York Bight from Long Island to Delaware Bay. Using the Doppler shifted radio signal scattered off the ocean surface [*Lipa and Barrick*, 1986], shore stations remotely obtain hourly surface current vector maps for most of the New Jersey shelf at approximately 6 km resolution, with increased resolution near the Hudson River mouth. These systems have been continuously operated since 1998 supporting validation [*Kohut and Glenn*, 2003; *Kohut et al.*, 2006b] and process studies across the shelf [*Chant et al.*, 2004; *Kohut et al.*, 2004, 2006a; *Oliver et al.*, 2004; *Ullman et al.*, 2006].

[9] The surface circulation is also illustrated by using near-surface drifters. The drifters were Self-Locating Datum Marker Buoys (SLDMBs) provided by the United States Coast Guard Office of Search and Rescue. The drifters are drogued at the upper 1 m of the water column and tracked via satellite. Seven drifters were released in the southern flank of the Hudson Shelf Valley on 26 July 2006 (day 207) in two clusters. The inshore cluster contained four drifters and was released at the 36 m isobath, while the offshore cluster, containing 3 drifters, was released at the 55 m isobath.

[10] Winds were measured at the NOAA National Data Buoy Center (NDBC) buoy 44025 located at 40.25°N, 73.17°W (see Figure 1 for location). Neutral wind stress was calculated following *Large and Pond* [1981] and then low-pass filtered (half-power point of 40 h) to remove short-period fluctuations (Figure 2). Gaps in the NOAA NDBC buoy 44025 record were filled through regression with the nearby NOAA CMAN station at Ambrose Light (40.46°N, 73.83°W).

[11] Freshwater discharge in the region is dominated by the Hudson River. Daily values of discharge at Poughkeepsie, NY were obtained at the USGS website (http://waterdata.usgs.gov). The watershed upstream of Poughkeepsie is approximately 10% less than the total Hudson River watershed [*Chant et al.*, 2008], so the actual total discharge is presumably about 10% larger than reported here (Figure 2). Daily values of the Connecticut River discharge at Thompsonville, CT were also obtained (Figure 2).

3. Results

3.1. Temporal Evolution of Winds and Freshwater Content Over the Shelf

[12] The wind stress during spring and summer 2006 exhibited the typical ''weather band'' variability, with fluctuations of the order of a few days (Figure 2). Winds oscillate frequently between upwelling and downwelling favorable from early April to mid May. After that, winds become predominantly upwelling favorable, with only a few downwelling favorable wind events occurring until September. The cumulative wind stress, shown here to more clearly indicate the upwelling season, increases nearly monotonically during this period. September and October are also characterized by predominantly upwelling favorable winds, but the frequency and intensity of downwelling

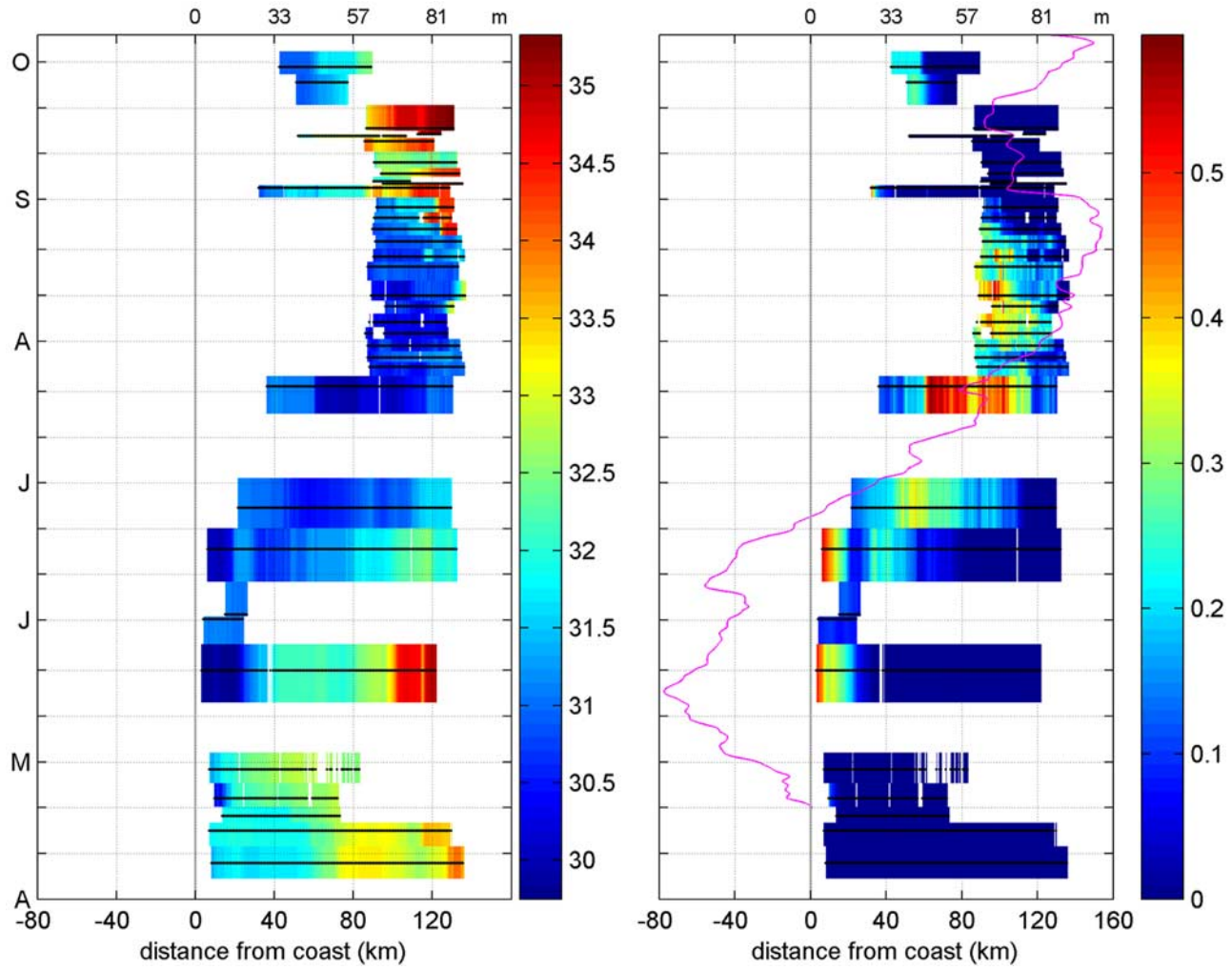

Figure 3. Time evolution of (left) surface salinity and (right) equivalent depth of freshwater (in meters) as a function of distance from the coast along the Endurance Line (see Figure 1 for location) off New Jersey. The water depth at some locations along the Endurance Line is shown on the top of each panel. The magenta curve on the right is the excursion length (*Le*) of the plume (see equation (2) for definition), which is exactly proportional to the cumulative wind stress shown in Figure 2. Black horizontal lines show time and location of measurements, and the gray line indicates the coast.

events increase, leading to only small changes in the cumulative wind stress.

[13] The Hudson River historical average peak discharge occurs in late March/early April. In 2006, after a large discharge pulse in January (not shown), the river discharge consists of relatively small pulses until late April (Figure 2), when a large discharge event occurs. The 'background' discharge is higher (about 1000 m^3s^{-1}) from mid May to early August, with a very large pulse occurring in late June. The peak in late June was the fifth largest discharge event in the USGS record at Cohoes that dates back to 1918, and the fourth largest at Fort Edward, which dates back to 1976. From August to November, the discharge from 2006 agrees relatively well with climatology, i.e., very low discharge during late summer, increasing toward the end of the year. The Connecticut River discharge presents a similar pattern. The discharge from early May to mid June is comparable to the Hudson River discharge. After that, however, the Connecticut River discharge is smaller, generally by a factor of 2. The event in late June, in particular, is significantly smaller than in the Hudson River.

[14] The temporal evolution of surface salinity and equivalent depth of freshwater along the Endurance Line (see Figure 1 for location) is shown in Figure 3. The equivalent depth of freshwater (*Fs*, in meters) is defined as

$$Fs = \int_{-h}^{0} \frac{S_0 - S(z)}{S_0} dz \qquad (1)$$

where z is the vertical coordinate, S is the salinity of the water column measured with the gliders, S_0 is the value of the reference salinity and h is the depth at which it occurs. Analyses of vertical sections of salinity measured with the glider suggest a reference value of 31.5 for the surface layer of freshwater. Qualitatively similar results are obtained if a reference value of 32 is used.

[15] The surface salinity exhibits strong seasonal variability, with the freshest water occurring during summer. Early

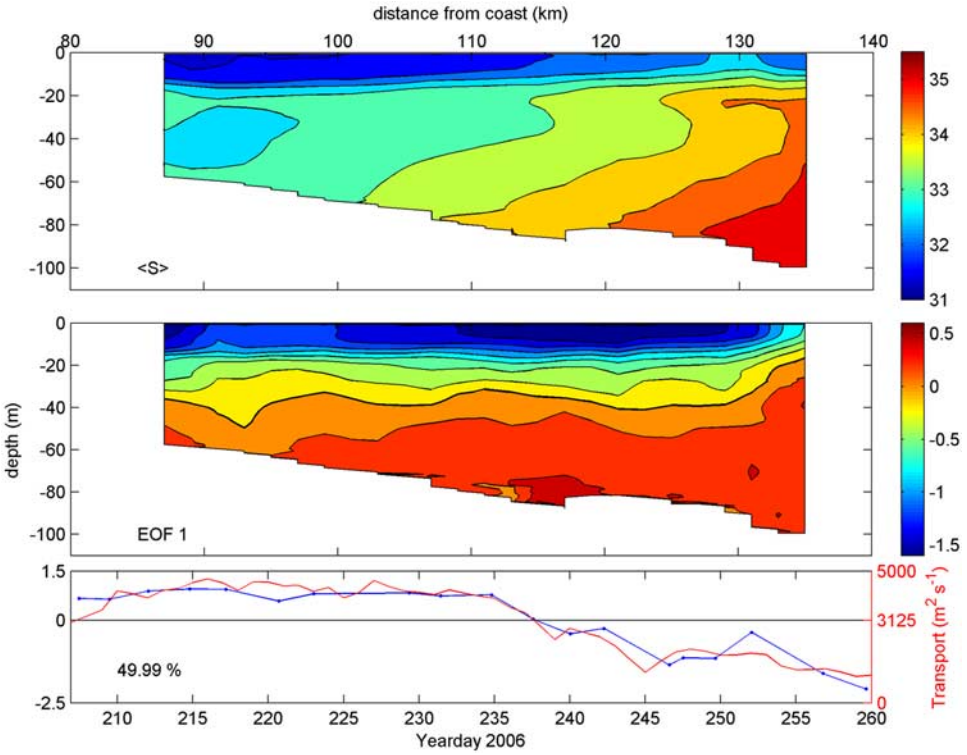

Figure 4. (top) Average salinity along the Endurance Line from 26 July (day 207) to 17 September (day 260), (middle) the first empirical orthogonal function (EOF) and (bottom) the amplitude time series of the first EOF mode of the salinity field (blue). The percentage of the total variance explained by the first EOF mode is shown. Red line is the surface transport time series based on CODAR measurements through the transect shown in Figure 6b. The same time series for the entire study period is shown in Figure 8. See section 3.3 for details.

in the year, salinity is generally lower close to the coast, increasing nearly monotonically in the offshore direction. Salinity is everywhere higher than 31.5, so *Fs* is zero throughout the shelf. From mid May to mid June, salinity close to the coast drops considerably. This is presumably due to the increase in the Hudson River discharge that occurs in late April, as the freshwater is transported downstream from the river mouth in a coastal current. The equivalent depth of freshwater is high in a thin band roughly 10–15 km wide close to the coast, decreasing rapidly offshore. This pattern changes as the season progresses, and the region with freshwater widens significantly, spanning the entire shelf during summer. Low salinity waters can be found at about 120 km from the coast for almost 2 months, from late June to late August. Observations during part of that period are restricted to the offshore region, and no information is available inshore of the 60 m isobath. During late August/early September, salinity in the offshore region increases rapidly, and the fresher water seems again to be restricted to being close to shore after that. A similar seasonal variation is observed in glider data collected in 2004 [*Castelao et al.*, 2008], with the region with freshwater beginning to widen in May, and thinning in September/October.

[16] The persistent occurrence of a fresher surface layer offshore during late July to mid August is clearly seen in the first empirical orthogonal function (EOF) of the salinity vertical sections (Figure 4). Only data from 26 July (day 207) to 17 September (day 260) were used in the computation, since the frequency of observations was highest during this period. The first mode, which explains 50% of the total variance, is characterized by large negative values in the top layer, and small positive values near the bottom. The amplitude time series (blue line in the bottom panel) is positive until 23 August (day 235), representing a substantial decrease in the surface salinity compared to the average field (top panel). From that point on, the amplitude decreases rapidly and remains negative, indicating a salinity increase of about 2–2.5 in the surface layer.

[17] Perhaps the most remarkable feature in the temporal evolution of the surface salinity is the occurrence of large lenses of freshwater in the offshore region during late July to late August. For example, the equivalent depth of freshwater is higher than 0.45 m for over 40 km on 22 July (day 203, Figures 3 and 5). This freshwater lens is possibly a result of the very large river discharge event that occurred in late June. Significant cross-shelf transport of the Hudson's outflow is apparent again on 11 August (day 223), as a freshwater lens reached the 70 m isobath. Vertical sections of temperature and salinity were used to estimate the density anomaly ($\Delta\rho$) of these freshwater lenses. Here we define $\Delta\rho$ as the difference between the average density of a particular lens and the density of the surrounding ambient water (ρ_o). We compute ρ_o based on observations from the upper water column ($S < 31.5$), above the halocline, since the density from waters below reflects other features/processes, like the pres-

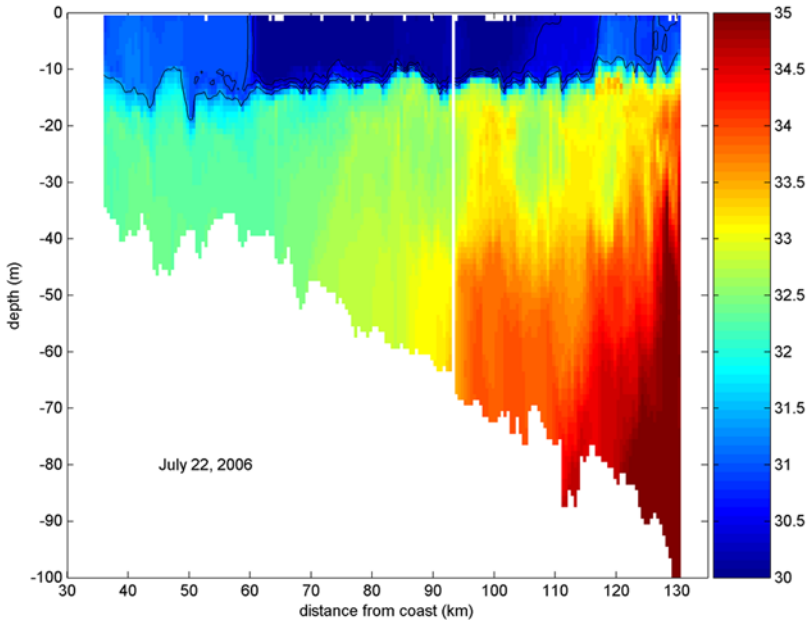

Figure 5. Salinity cross section on 22 July (day 203). Contours shown are 30.5, 31, and 31.5.

ence of the cold pool, migrations in the position of the shelf slope front, etc. The background density ρ_o is influenced by waters of Artic origin that are advected into the Middle Atlantic Bight [*Chapman and Beardsley*, 1989].

[18] The large lens observed on 22 July (day 203) and shown in Figures 3 and 5 ($Fs > \sim 0.45$ m) has a density anomaly $\Delta\rho = 0.67$ kg m^{-3}. A similar density anomaly ($\Delta\rho = 0.68$ kg m^{-3}) is observed for the lens on 11 August (day 223). We emphasize that this is the density anomaly between the freshwater lens and the surrounding surface water. In the following sections, we explore the different cross-shelf transport mechanisms that could explain the occurrence of those freshwater lenses with large density anomaly in the offshore region.

3.2. Cross-Shore Transport Via Ekman Dynamics

[19] Upwelling favorable along-shelf winds oppose the along-shelf propagation of buoyancy-driven coastal currents and can inhibit their formation [e.g., *Chao*, 1988; *Kourafalou et al.*, 1996a, 1996b; *García Berdeal et al.*, 2002; *Lentz and Largier*, 2006]. Numerical simulations of the Hudson River outflow suggest that even weak to moderate upwelling winds can prevent the formation of a buoyant coastal current in the region [*Choi and Wilkin*, 2007]. If a buoyant coastal current already exists at the onset of upwelling winds, however, the wind-driven Ekman transport can advect the freshwater offshore in the surface layer [e.g., *Fong et al.*, 1997; *Hickey et al.*, 1998, 2005; *Fong and Geyer*, 2001; *García Berdeal et al.*, 2002; *Lentz*, 2004], being potentially an important mechanism for the cross-shelf transport of freshwater across the shelf. The excursion length of the plume (*Le*) is given by *Fong et al.* [1997]

$$Le(t) = \int_0^t u \quad dt = \int_0^t \frac{\tau}{\rho f D} dt \qquad (2)$$

where u is the Ekman driven velocity in the surface layer ($u = \tau/(\rho f D)$), τ is the along-isobath wind stress (27° clockwise from north), D is the depth at which the stress vanishes, and f is the Coriolis parameter. The thickness of the surface layer above the pycnocline during summer 2006, based on the in situ observations, was about 10 m. Using this average thickness as D, and the wind stress time series plotted in Figure 2, the time series of *Le* was computed (Figure 3). Note that the initial value of *Le* is arbitrary, i.e., the curve can be shifted unrestrictedly in the cross-shore direction. The difference between *Le* at two different times gives the Ekman driven excursion of a plume during that period. The slope of *Le* is consistent with the widening of the region with freshwater over the shelf, suggesting Ekman dynamics might be important in the process.

[20] The offshore edge of the freshwater lenses found on 22 July (day 203) and 11 August (day 233) are located at about 100 and 95 km from the coast, respectively. That means the lenses must have been advected across the shelf for approximately 85–90 km, if they are indeed the result of offshore transport of buoyant water from the coastal current ($\sim$10 km wide) in the surface layer. The time series of *Le* indicates that the time necessary for that excursion is about 30 d. If D is assumed to be 5 m, a small value compared to observations, the excursion time would be about 15 d in both cases.

[21] The scenario in which buoyant water is transported offshore by upwelling favorable winds was explored in great detail by *Fong and Geyer* [2001] and *Lentz* [2004]. They showed that, while the plume is advected offshore, it is susceptible to significant mixing. Therefore if this is the mechanism responsible for carrying the freshwater lenses offshore during SW06, we expect a significant dilution of the plume in the process. *Lentz* [2004] developed a two-dimensional model that provides an estimation of the plume density change in response to winds, and compares well with numerical model results and observations. The reader is referred to *Lentz* [2004] for details of the model.

[22] Although the model represents a simplified scenario, we use it to estimate the expected amount of dilution of the plume as it is advected offshore in the surface Ekman layer. The plume thickness at the coast is set to 10 m, the plume width at the surface is considered in the range 1–15 km, and the model is forced with measured winds prior to 22 July (day 203). Model results show that after 15 d of wind-forcing, the density anomaly of the plume is about 8% of the value at the coast, and it is less than 4% after 30 d. A similar result is obtained for the freshwater lens on 11 August (day 223), with an expected dilution to 6–12% of the original density anomaly. Therefore the model indicates that the density anomaly at the coastal current needs to be very large in order for this mechanism to explain the occurrence of the freshwater lenses offshore. The large density anomalies needed at the coast are not supported by observations. We emphasize, however, that several potentially important processes that are not included in the model physics may be responsible for the discrepancy between the model predictions and the observations. One issue is that the model does not include a continuous source of freshwater, which would tend to freshen the plume and move the model predictions closer to the observations. We do note, however, that the outflow in late June and July was characterized by spikes followed by substantial reductions in discharge and thus we expect the influence of the continuous source to be smaller than that associated with a constant discharge. Nevertheless, this makes the comparison inconclusive in determining the direct impact of Ekman dynamics on the cross-shelf transport of the lenses.

3.3. Advection by Offshore Directed Jet

[23] In order to investigate if three-dimensional effects play an important role on the occurrence of the freshwater lenses, surface velocity maps derived from land-based coastal radar are used. Since the interest is in advection of the buoyant water, it is important to look at the history of the velocity over the previous days. The surface velocity is, therefore, convoluted with a one-sided, exponentially decaying filter

$$v_k(t) = \frac{\int_{-\infty}^{t} v(t')e^{(t'-t)/k}dt'}{\int_{-\infty}^{t} e^{(t'-t)/k}dt'} \quad (3)$$

where k is a decay scale and v is a velocity component. k is chosen to be 14 d, since that is the time needed for typical 0.1 ms^{-1} shelf currents to advect waters from the river mouth to the SW06 region. Plots of $\mathbf{v_{14}}$ on 22 July (day 203) and 11 August (day 223), the time of the observation of the freshwater lenses discussed in sections 3.1 and 3.2, are shown in Figure 6. On 22 July, $\mathbf{v_{14}}$ reveals the existence of a clear and distinct flow intensification directed toward the south, from 73.3°W, 40.2°N to the SW06 region. A similar feature is observed on 11 August, although slightly shifted to the south. The signature of the jet is very clear in the sea surface temperature satellite image from 12 August (day 224). A tongue of cold water being advected south from the Long Island coast to the SW06 region coincides with the location of the jet. The presence of this flow intensification is a robust feature, and it is still clearly observed even if much smaller values of the decay scale k are used in (3).

[24] Further evidence of the occurrence of the jet is provided by near-surface drifters, which are shown in Figure 7 four days after deployment. For consistency, $\mathbf{v_4}$, rather than $\mathbf{v_{14}}$, is also plotted. Note that the velocity pattern is similar if $\mathbf{v_{14}}$ is used, with the exception that in the latter case the velocity magnitudes are smaller. The jet on 30 July (day 211) is more directed offshore than in the other two examples shown in Figure 6, illustrating its time variability. The drifters' trajectories are in close agreement with the surface velocity measurements. The inshore cluster first moves north before turning offshore, while the offshore cluster moves almost in a straight line toward the shelf break. The drifters' trajectories are approximately 90° to the right of the average wind stress direction during the four days. The near-surface drifters are drogued at the upper 1 m of the water column, where Ekman velocities are expected to be at an angle significantly less than 90° because the drifters occupy merely the upper 10% of the Ekman layer. This suggests it is unlikely that the near-surface trajectories are just due to Ekman surface currents. The drifters' trajectories also exhibit shorter timescale variability, possibly due to inertial oscillations and tidal effects, which are not observed in the filtered velocities. After 30 July, the jet moves slightly south (see position on 11 August, day 223, Figure 6b), leaving the drifters in deeper waters to the east.

[25] A time series of the transport perpendicular to a transect across the jet in the surface layer (in units of $m^2\ s^{-1}$, positive means flow to the south and offshore, see Figure 6b for transect location) shows that the jet transport is not very sensitive to the decay scale used, as revealed by the similarity between the time series with k = 8 and 14 d. The time series reveal that the jet is present during most of summer. A three to four and a half-fold increase in the transport is observed from late June to late August compared to earlier in the year. This is roughly the same period the freshwater lenses are found in the offshore region (Figure 3). In particular, the most frequent observation of the lenses (early August) occurs when the jet transport is at its peak, and the river discharge is still relatively high. There is a rapid drop in the transport from 23 August (day 235) to 2 September (day 245), a period when the river discharge is low. During that period, the surface salinity in the offshore region increases considerably (Figure 3). Note the agreement between the timing of the decrease in the amplitude time series of the first EOF of the salinity field and the decrease in the jet transport (Figure 4). These results suggest the jet can provide an important and direct pathway for transporting freshwater and the material it contains from the river mouth vicinity across the shelf.

Figure 6. Averaged surface velocity ($\mathbf{v_{14}}$, see equation (3) for definition) on (a) 22 July (day 203) and (b) 11 August (day 223). Velocities on 11 August are overlain on sea surface temperature (°C) image from 12 August (day 224). No image is available for 22 July. The black line indicates the SW06 region, and the red line on the bottom panel is the transect used for computing the transport time series shown in Figures 4 and 8. Topographic contours as in Figure 1.

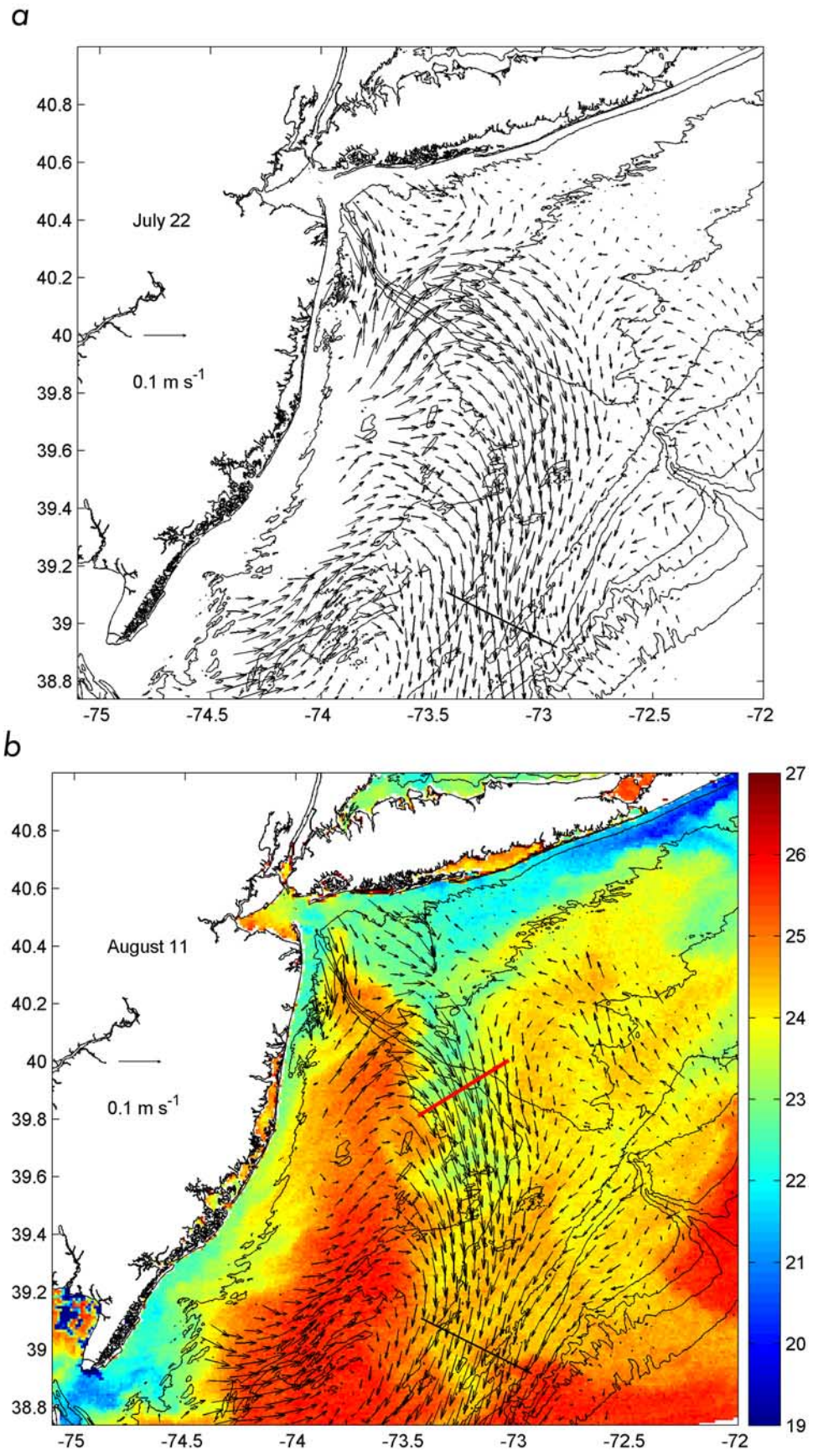
a
July 22
0.1 m s-1
40.8
40.6
40.4
40.2
40
39.8
39.6
39.4
39.2
39
38.8
-75
-74.5
-74
-73.5
-73
-72.5
-72
b
August 11
0.1 m s-1
27
26
25
24
23
22
21
20
19

Figure 6

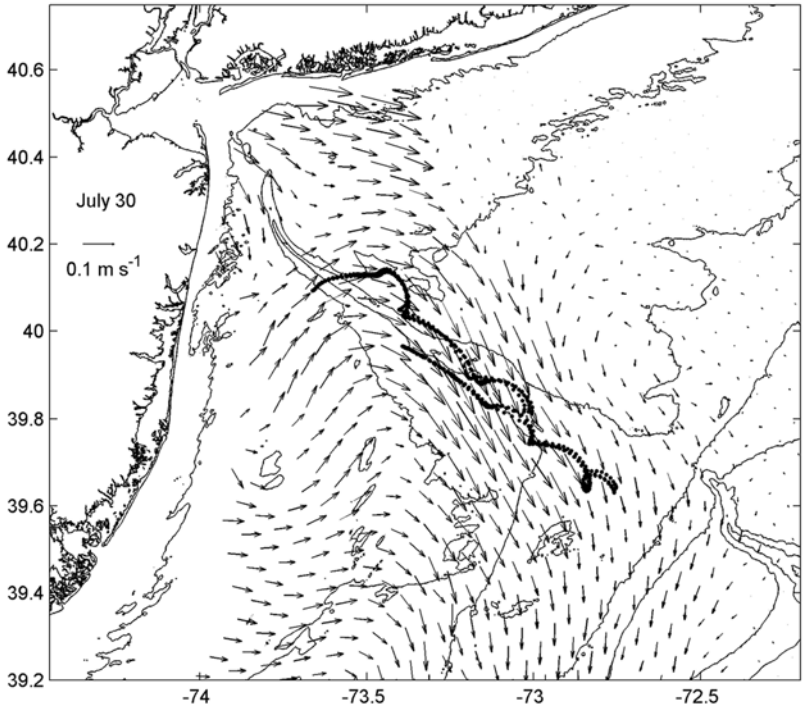

Figure 7. Averaged land-based surface velocity ($\mathbf{v_4}$, see equation (3) for definition) on 30 July (day 211), overlain with drifters' trajectories four days after deployment. Topographic contours as in Figure 1.

[26] The weighted averaged along-isobath wind stress [*Austin and Barth*, 2002], computed as in (3) but with the velocity replaced by the along-isobath wind stress, is also shown in Figure 8. Upwelling favorable winds are positive, while downwelling favorable winds are negative. There is a general tendency for increased jet transport during periods when the wind is upwelling favorable. Note that the jet is almost upwind during those periods. The correlation coefficient (CC) between the wind stress and the transport during 1 May (day 121) to 30 September (day 273) is significant at the 95% level as long as k is smaller than or equal to 4 d. For k = 4 d, CC = 0.68. As k increases above 4 d, the correlation increases but the drop in the effective number of degrees of freedom [*Emery and Thomson*, 2001] makes the correlation not significant at the 95% level. Although we cannot rule out the possibility of Ekman transport contributing to the correlation between the wind and the jet transport, the fact that the angle between the wind stress and the normal to the transect (i.e., the direction of the jet) is approximately 120° makes it unlikely that the velocities are directly driven by Ekman dynamics but rather involves a more complicated dynamics that may involve interactions with bottom topography. The details of these interactions are currently being addressed with numerical simulations [Zhang et al., personal communication].

4. Discussion and Conclusions

[27] The observations described in this paper reveal a strong seasonal variation in the freshwater content over the New Jersey shelf during 2006. Freshwater is restricted to a narrow band (~10 km) close to the coast during spring, but occupies the entire width of the shelf during July and

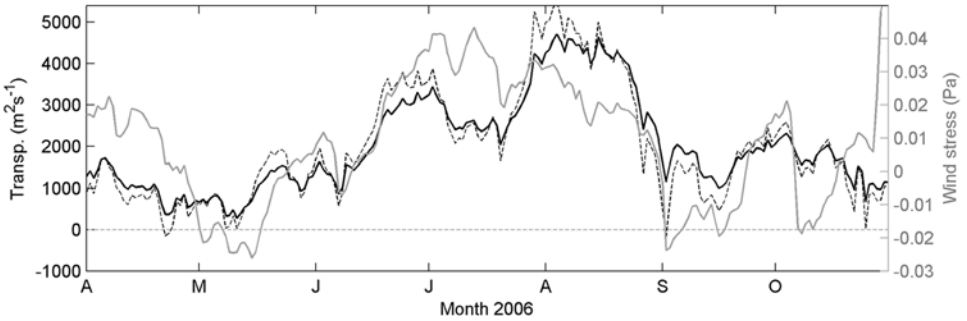

Figure 8. Time series of jet surface transport (m^2 s^{-1}, positive offshore and to the south) through transect shown in Figure 6b during 2006. Velocities computed as in equation (3), with decay scale of 8 (dashed black) and 14 (solid black) days. Also shown is the along-isobath wind stress with decay scale of 14 d (gray).

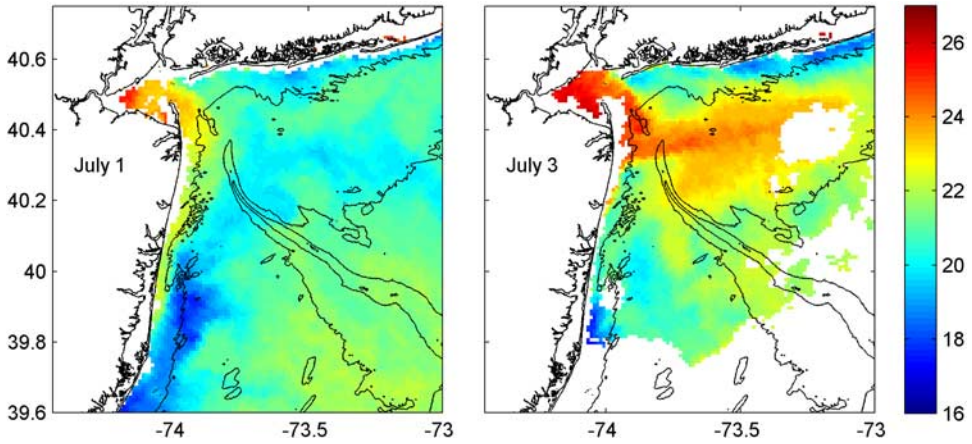

Figure 9. Sea surface temperature (°C) on 1 July (day 182) and 3 July (day 184), 2006. White areas are clouds.

August. During the latter period, lenses of freshwater with high density anomaly are found reaching about 100 km from the coast. Estimations of Ekman transport are consistent with the observed widening of the region with freshwater over the shelf. As freshwater is advected offshore, however, it is expected to mix with the ambient water, decreasing the density anomaly of the plume. Comparisons with a model based on Ekman dynamics [*Lentz*, 2004], using time-dependent measured winds, suggest that the density anomaly at the coast needed to explain the occurrence of the freshwater lenses in late July and early August is much larger than supported by observations. However, Ekman dynamics cannot be ruled out as a possible mechanism for transporting the lenses offshore, since some potentially important aspects are not resolved by the model.

[28] Regardless of the importance of Ekman dynamics, an alternative mechanism to transport the freshwater lenses with high density anomaly offshore is provided by analyses of surface velocities, satellite imagery and drifters' trajectories. Velocity observations during summer show the persistent occurrence of a flow intensification directed offshore and to the south, from about the 40 m isobath near the river mouth toward the SW06 region. Drifters' trajectories and sea surface temperature satellite observations provide further evidence of the jet. The present observations suggest the occurrence of the jet following a period of high river discharge as a possible mechanism for rapidly transporting the freshwater across the shelf. This is a different mechanism than the widely reported offshore advection due to surface Ekman transport [e.g., *Fong and Geyer*, 2001; *Lentz*, 2004; *Choi and Wilkin*, 2007].

[29] During high discharge events, bulge formation in the Hudson River mouth appears to be a robust feature [*Chant et al.*, 2008; O. Schofield et al., The Hudson River plume and its role in low dissolved oxygen on the Mid-Atlantic Bight, submitted to *J. Geophys. Res.*, 2008]. The growth of a bulge and accumulation of fluid within it has been shown to coincide with a reduction in buoyant coastal current transport to 30–50% of the inflow discharge [*Fong and Geyer*, 2002; *Horner-Devine et al.*, 2006; *Chant et al.*, 2008]. This is consistent with acoustic Doppler current profiler (ADCP) observations from a cable observatory located near Tuckerton, at about 10 km from the coast (Long-Term Ecosystem Observatory, LEO [*Grassle et al.*, 1998]). The ADCP record extends from 19 May (day 139) to 17 July (day 198). No noticeable increase in southward velocities is observed following the large discharge event that occurs in late June (not shown). As water accumulates near the mouth due to bulge formation during high discharge events, upwelling winds can help transport the freshwater from the river mouth to the region where the jet is found [see, e.g., *Choi and Wilkin*, 2007]. Evidence of that is provided by satellite imagery from early July (Figure 9) soon after the large river discharge event that occurred in late June. The wind at that time is predominantly upwelling favorable (Figures 2 and 8). The river plume is transported offshore as in the numerical simulations by *Choi and Wilkin* [2007] to the region where the jet is generally found. Once plume waters reach that location, the jet can provide an important and direct pathway for transporting freshwater and the material it contains, including phytoplankton, dissolved organic and nonalgal particulate matter, from the river mouth vicinity across the shelf. It is reasonable to think that the tongue of water coming from the Long Island near-coastal region on 12 August (day 224, Figure 6b) might be mostly formed by shelf waters. However, any freshwater from the Hudson River or from farther north (e.g., Connecticut River) that reaches the location where the jet is found will presumably be also advected across the shelf.

[30] The jet transport is significantly correlated with upwelling favorable winds on a scale of a few days. However, careful examination of the time series reveal that the weighted averaged winds during August, for example, are weaker than during July, but the transport in the jet is higher. This suggests other effects (e.g., stratification) are probably important in the dynamics of the jet. Indeed, upwelling winds and jet transport are correlated from May on (the same period when the Hudson River discharge increases), but not before that (January to April). There is no clear agreement between the timing of peaks in river discharge and jet transport (Figures 2 and 8), though. Analyses of previous CODAR observations suggest that the jet is present in other years, but more intermittently and somewhat weaker.

[31] The rapid cross-shelf transport of the Hudson River outflow is consistent with analysis by *Mountain* [2003] who

noted a significant annual cycle in the shelf salinity in the New York Bight Apex, and that this seasonal variability was absent to the south off Delaware and Chesapeake Bays. Mountain's results were based on coarse CTD surveys that we suggest may have missed the seasonal freshwater signal discharging from the Delaware and Chesapeake Bays that may have been largely contained in a narrow coastal current. In contrast, due to the rapid cross-shelf spreading of the Hudson River outflow, the coarse CTD surveys were able to pick up the Hudson's annual freshwater signal.

[32] Finally, we note that the dynamics of the jet are currently not understood. Understanding its dynamics, including forcing mechanisms and timescales of variability, is a crucial step for improving the understanding of the transport pathways of the Hudson River plume on the New Jersey shelf.

[33] **Acknowledgments.** We are grateful to Steve Lentz and two anonymous reviewers for their comments and suggestions, which led to an improved manuscript. We also thank Steve for kindly providing the codes with the implementation of his model. We thank the members of the Rutgers University Coastal Ocean Observation Laboratory, who were responsible for the highly successful glider operations. John Kerfoot, Jennifer Bosch, and Sage Lichtenwalner helped with data collection and processing. Some of the glider observations used in this study were collected by the Oregon State University glider group. We thank Kipp Shearman and Jack Barth for graciously providing those observations. The United States Coast Guard Office of Search and Rescue provided the drifters used in this study. This research was supported by the Nonlinear Internal Waves Initiative component of the Office of Naval Research's Shallow Water 2006 Joint Experiment (grant N000140610283), by ONR under grant N000140610739, and by the National Science Foundation under grant OCE 0238957. The observatory data used was supported by ONR, NSF, NOAA, NOPP, DHS, DoD, and the State of NJ. Oregon State University glider observations were supported by ONR (grant N000140610282).

References

Austin, J. A., and J. A. Barth (2002), Variation in the position of the upwelling front on the Oregon shelf, *J. Geophys. Res.*, *107*(C11), 3180, doi:10.1029/2001JC000858.

Avicola, G., and P. Huq (2003), The role of outflow geometry in the formation of the recirculating bulge region in coastal buoyant outflows, *J. Mar. Res.*, *61*, 435–463.

Barrick, D. E., M. W. Evens, and B. L. Weber (1977), Ocean surface currents mapped by radar, *Science*, *198*, 138–144.

Blumberg, A. F., L. A. Khan, and J. P. St. John (1999), Three-dimensional hydrodynamic model of New York Harbor region, *J. Hydraul. Eng.*, *125*, 799–816.

Castelao, R. M., S. Glenn, O. Schofield, R. Chant, J. Wilkin, and J. Kohut (2008), Seasonal evolution of hydrographic fields in the central Middle Atlantic Bight from glider observations, *Geophys. Res. Lett.*, *35*, L03617, doi:10.1029/2007GL032335.

Chant, R. J., S. M. Glenn, and J. Kohut (2004), Flow reversals during upwelling conditions on the New Jersey inner shelf, *J. Geophys. Res.*, *109*, C12S03, doi:10.1029/2003JC001941.

Chant, R. J., S. M. Glenn, E. Hunter, J. Kohut, R. F. Chen, R. W. Houghton, J. Bosch, and O. Schofield (2008), Bulge formation of a buoyant river outflow, *J. Geophys. Res.*, *113*, C01017, doi:10.1029/2007JC004100.

Chao, S.-Y. (1988), Wind-driven motion of estuarine plumes, *J. Phys. Oceanogr.*, *18*, 1144–1166.

Chapman, D. C., and R. C. Beardsley (1989), On the origin of shelf water in the Middle Atlantic Bight, *J. Phys. Oceanogr.*, *19*, 384–391.

Choi, B.-J., and J. L. Wilkin (2007), The effect of wind on the dispersal of the Hudson River plume, *J. Phys. Oceanogr.*, *37*, 1878–1897.

Csanady, G. T. (1978), Wind effects on surface to bottom fronts, *J. Geophys. Res.*, *83*(C9), 4633–4640.

Emery, W. J., and R. E. Thomson (2001), *Data Analysis Methods in Physical Oceanography*, 2nd edition, 638 pp., Elsevier, Amsterdam.

Fofonoff, P., and R. C. Millard (1983), Algorithms for computation of fundamental properties of seawater, *UNESCO Tech. Pap. Mar. Sci.*, *44*, 53 pp.

Fong, D. A., and W. R. Geyer (2001), Response of a river plume during an upwelling favorable wind event, *J. Geophys. Res.*, *106*(C1), 1067–1084.

Fong, D. A., and W. R. Geyer (2002), The alongshore transport of freshwater in a surface-trapped river plume, *J. Phys. Oceanogr.*, *32*, 957–972.

Fong, D. A., W. R. Geyer, and R. P. Signell (1997), The wind-forced response of a buoyant coastal current: Observations of the western Gulf of Maine plume, *J. Mar. Syst.*, *12*, 69–81.

García Berdeal, I., B. M. Hickey, and M. Kawase (2002), Influence of wind stress and ambient flow on a high discharge river plume, *J. Geophys. Res.*, *107*(C9), 3130, doi:10.1029/2001JC000932.

Garvine, R. W. (1995), A dynamical system for classifying buoyant coastal discharges, *Cont. Shelf Res.*, *15*, 1585–1596.

Garvine, R. W. (1999), Penetration of buoyant coastal discharge onto the continental shelf: A numerical model experiment, *J. Phys. Oceanogr.*, *29*, 1892–1909.

Geyer, W. R., J. H. Trowbridge, and M. M. Bowen (2000), The dynamics of a partially mixed estuary, *J. Phys. Oceanogr.*, *30*, 2035–2048.

Grassle, J. F., S. M. Glenn, and C. von Alt (1998), Ocean Observing Systems For Marine Habitats, paper presented at Ocean Community Conference '98, Sea Technology, Washington, Nov.

Hallock, Z. R., and G. O. Marmorino (2002), Observations of the response of a buoyant estuarine plume to upwelling favorable winds, *J. Geophys. Res.*, *107*(C7), 3066, doi:10.1029/2000JC000698.

Hickey, B. M., L. J. Pietrafesa, D. A. Jay, and W. C. Boicourt (1998), The Columbia River plume study: Subtidal variability in the velocity and salinity fields, *J. Geophys. Res.*, *103*(C5), 10,339–10,368.

Hickey, B. M., S. Geier, N. Kachel, and A. MacFadyen (2005), A bidirectional river plume: The Columbia in summer, *Cont. Shelf Res.*, *25*, 1631–1656.

Horner-Devine, A. R., D. A. Fong, S. G. Monismith, and T. Maxworthy (2006), Laboratory experiments simulating a coastal river inflow, *J. Fluid Mech.*, *555*, 203–232.

Johnson, D. R., A. Weidemann, R. Armone, and C. O. Davis (2001), Chesapeake Bay outflow plume and coastal upwelling events: Physical and optical properties, *J. Geophys. Res.*, *106*(C6), 11,613–11,622.

Johnson, D. R., J. Miller, and O. Schofield (2003), Dynamics and optics of the Hudson River outflow plume, *J. Geophys. Res.*, *108*(C10), 3323, doi:10.1029/2002JC001485.

Kohut, J. T., and S. M. Glenn (2003), Improving HF radar surface current measurements with measured antenna beam patterns, *J. Atmos. Oceanic Technol.*, *20*, 1303–1316.

Kohut, J. T., S. M. Glenn, and R. J. Chant (2004), Seasonal current variability on the New Jersey inner shelf, *J. Geophys. Res.*, *109*, C07S07, doi:10.1029/2003JC001963.

Kohut, J. T., S. M. Glenn, and J. D. Paduan (2006a), Inner shelf response to Tropical Storm Floyd, *J. Geophys. Res.*, *111*, C09S91, doi:10.1029/2003JC002173.

Kohut, J., H. Roarty, and S. M. Glenn (2006b), Characterizing observed environmental variability with HF Doppler radar surface current mappers and acoustic Doppler current profilers: Environmental variability in the coastal ocean, *IEEE J. Oceanic Eng.*, *31*, 876–884, doi:10.1109/JOE.2006.886095.

Kourafalou, V. H., L.-Y. Oey, J. D. Wang, and T. N. Lee (1996a), The fate of river discharge on the continental shelf: 1. Modeling the river plume and the inner shelf coastal current, *J. Geophys. Res.*, *101*(C2), 3415–3434.

Kourafalou, V. H., T. N. Lee, L.-Y. Oey, and J. D. Wang (1996b), The fate of river discharge on the continental shelf: 2. Transport of coastal low-salinity waters under realistic wind and tidal forcing, *J. Geophys. Res.*, *101*(C2), 3435–3455.

Large, W., and S. Pond (1981), Open ocean momentum flux measurements in moderate to strong winds, *J. Phys. Oceanogr.*, *11*, 314–336.

Lentz, S. (1995), U.S. contributions to the physical oceanography of continental shelves in the early 1990's, *Rev. Geophys.*, *33*(S1), 1225–1236.

Lentz, S. (2004), The response of buoyant coastal plumes to upwelling-favorable winds, *J. Phys. Oceanogr.*, *34*, 2458–2469.

Lentz, S., and J. Largier (2006), The influence of wind forcing on the Chesapeake Bay buoyant coastal current, *J. Phys. Oceanogr.*, *36*, 1305–1316.

Lipa, B. J., and D. E. Barrick (1986), Extraction of sea state from HF-radar sea echo: Mathematical theory and modeling, *Radio Sci.*, *21*, 81–100.

Mountain, D. G. (2003), Variability in the properties of Shelf Water in the Middle Atlantic Bight, 1977–1999, *J. Geophys. Res.*, *108*(C1), 3014, doi:10.1029/2001JC001044.

Munchow, A., and R. W. Garvine (1993), Buoyancy and wind forcing of a coastal current, *J. Mar. Res.*, *51*, 293–322.

Oliver, M., J. Kohut, A. Irwin, O. Schofield, S. M. Glenn, M. A. Moline, and W. P. Bissett (2004), Bioinformatic approaches for objective detection of water masses, *J. Geophys. Res.*, *109*, C07S04, doi:10.1029/2003JC002072.

Peters, H. (1999), Spatial and temporal variability of turbulent mixing in an estuary, *J. Mar. Res.*, *57*, 805–845.

Rennie, S., J. L. Largier, and S. J. Lentz (1999), Observations of low-salinity coastal current pulses downstream of Chesapeake Bay, *J. Geophys. Res.*, *104*(C8), 18,227–18,240.

Sanders, T. M., and R. W. Garvine (2001), Freshwater delivery to the continental shelf and subsequent mixing: An observational study, *J. Geophys. Res.*, *106*(C11), 27,087–27,101.

Schofield, O., et al. (2007), Slocum gliders: Robust and ready, *J. Field Robotics*, *24*, 1–14, doi:10.1009/rob.20200.

Ullman, D. S., J. O'Donnell, J. Kohut, T. Fake, and A. Allen (2006), Trajectory prediction using HF radar surface currents: Monte Carlo simulations of prediction uncertainties, *J. Geophys. Res.*, *111*, C12005, doi:10.1029/2006JC003715.

Warner, J. C., W. R. Geyer, and J. A. Lerczak (2005), Numerical modeling of an estuary: A comprehensive skill assessment, *J. Geophys. Res.*, *110*, C05001, doi:10.1029/2004JC002691.

Yankovsky, A., and D. C. Chapman (1997), A simple theory for the fate of buoyant coastal discharges, *J. Phys. Oceanogr.*, *27*, 1386–1401.

R. Castelao, R. Chant, S. Glenn, J. Kohut, and O. Schofield, Institute of Marine and Coastal Sciences, Rutgers University, 71 Dudley Road, New Brunswick, NJ 08901, USA. (castelao@marine.rutgers.edu)